A. Bianconi (ed.) Symmetry and Heterogeneity in High Temperature Superconductors, 133-146
NATO Science Series II Mathematics,Physics and Chemistry – Vol. 214

III.3

STRUCTURAL SYMMETRY, ELASTIC COMPATIBILITY, AND THE INTRINSIC HETEROGENEITY OF COMPLEX OXIDES

S. R. Shenoy[1], T. Lookman[2], A. Saxena[2], and A. R. Bishop[2]
[1]International Centre for Theoretical Physics Trieste, Italy; [2]Los Alamos National Lab, Los Alamos, N.M., USA

Abstract: Intrinsic heterogeneity, from nano- to meso- scales, of lattice/charge/spin variables, is common in complex oxides such as cuprates and manganites, that have strain-based ferroelastic transitions. We summarize our viewpoint that the central player is the power-law, anisotropic, strain-strain force that lies concealed in the apparently innocuous St. Venant compatibility constraint, namely the maintenance of lattice integrity, under strain texturing induced by charges and spins, that act as 'local stresses' and 'local transition temperatures'

Key words: Transition Metal Oxides, Elasticity, Compatibility, Cuprates, Manganites

1. INTRINSIC HETEROGENEITY

In complex electronic oxides such as cuprates and manganites, a variety of finescale probes have revealed an unsuspected nanoworld of correlated multiscale spatial patterning in lattice structure, charge density/mobility, and staggered/direct magnetization [1,2,3]. These sign-varying patterns or 'textures' have been referred to as stripes, islands, nanoscale phase-separations, etc. Interestingly, there are both direct and *cross*-responses to external fields; and local responses to global perturbations. Thus, in

manganites not only does magnetic field change (colossally [1]) the resistance, but so does external stress [4]; and moreover a uniform field can induce nanoscale 'cloudlike' variations in the local conductance [5]. In cuprates (with an antiferromagnetic parent compound) a uniform magnetic field can orient mesoscale structural twins [6]. This argues for a multivariable cross-coupling: so external stress changes strain, that changes magnetization coupled to it; and similarly for other variables. Clearly an internal charge variation can act as an internal stress and affect the spins. The resultant self-consistent equilibrium state is not necessarily uniform. The *annealed*-variable inhomogeneities that may emerge from this internal coupling will here be termed 'intrinsic', distinguishing them from quenched-variable 'extrinsic' inhomogeneities also unavoidably present in the (usually nonstoichiometric) complex oxides. The fact that uniform fields can induce locally varying *multiscale* response argues for nonlinearities in at least one of these component variables, and so in Fourier space the resultant coupling of wave vectors interlinks the hierarchy of spatial (and temporal) scales.

Some of the extensive experimental and theoretical literature has been cited elsewhere [1,2]. Here, we focus on our own viewpoint regarding the underlying cause of these intrinsic inhomogeneities/heterogeneities [7-12]. The natural prejudice in favour of electronic/structural/magnetic states that are uniform at equilibrium, arises from the positive sign of gradient-squared terms: an initially random state flows energetically downhill by smoothing out spatial variations at all wavelengths. There are two exceptions to this: Nonlinear systems can have domains of competing ground states, with domain walls dividing the system–once formed, the nonuniform states are stable; and long-range forces competing with short-range couplings are well known to be able to induce nonuniform states. (Indeed, some models for stripes have invoked isotropic long-ranged Coulomb forces.) Our own Ginzburg-Landau model has *both* generic sources of nonuniformity. Apart from local couplings of charge and spin to strains, it has (structural-transition) nonlinearities in order-parameter strains; and purely local harmonic terms in other strains that, after enforcing a lattice integrity constraint [13-15], effectively become *anisotropic* long-range potentials. Our work explores the possibility that the constrained nonlinear system spontaneously forms multivariable inhomogeneous states, even without quenched disorder.

The key theoretical idea is to work in the *strain* representation [7-12,15] and impose the constraint of lattice integrity at all scales, through the St.

Venant compatibility (differential) equations for the strain-tensor components [14]. Elimination of some harmonic contributions in the free energy to satisfy the compatibility constraint leads to power-law anisotropic (PLA) potentials between the remaining order-parameter strain components, that vary directionally in sign [7,16]. Hence a local strain can receive conflicting ('ferro/antiferro') instructions from surrounding and even far-off strains, in a kind of elastic 'frustration' facilitating a structural patterning, and generating configurational glass-like multiple minima (a "landscape") in the space of all such possible states. Other variables coupled to lattice strains will also show sign-varying patterns or 'textures', through induced St. Venant PLA interactions. Thus in our scenario, strain modulations of an anisotropic, nonlinear, and non-ruptured lattice occur in its response to multiple local nanostresses exerted by the charges and spins; and these in turn, have density-wave modulations induced by the lattice strain textures [10,11]. The self-consistent multi-variable equilibrium states in doped ferroelastics such as the complex oxides can be intrinsically heterogeneous.

2. LATTICE HAMILTONIANS: SPRINGS AND STRAINS

As noted elsewhere [11], it is useful to classify *levels* of description through inverse wave vector scales $\lambda \equiv k^{-1}$, of solids with system size L_o, Bravais lattice until-cell a_o, and atomic basis scale l_o. Level 0 is the $\lambda \leq L_o$ scale of engineering mechanics; Level 1 is the (large) range of lattice strain variations $L_o > \lambda > a_o$; Level 2 is the intra-cell bond-stretching and bending or 'microstrain' range $a_o > \lambda > l_o$; and Level 3 is the electronic orbital scale $l_o > \lambda$. Consider for simplicity a 2D square unit-cell lattice $a_o \equiv 1$, with a monatomic basis at positions $\{\vec{R}_i\}$. Then the general interatomic potential energy is $V = (1/2)\sum_{i,j} V(\vec{R}_i - \vec{R}_j) = (1/2)\sum_{i,j} V(\vec{r}_i - \vec{r}_j + \vec{u}(\vec{r}_i) - \vec{u}(\vec{r}_j))$ where i th atomic positions displaced from reference lattice sites $\{\vec{r}_i\}$ are $\vec{R}_i = \vec{r}_i + u(\vec{r}_i)$. Taylor expanding in the displacement differences with $\vec{\Delta}$ the discrete difference operator $\Delta_\mu f(\vec{r}) \equiv f(\vec{r} + \hat{\mu}) - f(\vec{r})$ and $\hat{\mu} = \hat{x}, \hat{y}$, and with nearest-neighbour couplings only retained,

$$V \simeq (1/2)\sum_i \sum_{\substack{\mu\mu' \\ \nu\nu'}} C_{\mu\nu,\mu'\nu'}\Delta_\mu u_\nu \Delta_{\mu'} u_{\nu'} + ... = (1/2)\sum_i \sum_{\substack{\mu\mu' \\ \nu\nu'}} C_{\mu\nu,\mu'\nu'} E_{\mu\nu} E_{\mu'\nu'} + ... \qquad (1)$$

where with symmetric 'spring constant' coefficients $C_{\mu\nu,\mu'\nu'}$ it is convenient to define a symmetric *strain tensor* that in coordinate and Fourier space is

$$E_{\mu\nu}(\vec{r}) \equiv (1/2)[\Delta_\mu u_\nu(\vec{r}) + \Delta_\nu u_\mu(\vec{r})]\,; E_{\mu\nu}(k) \equiv (i/2)[K_\mu u_\nu(\vec{k}) + K_\nu u_\mu(\vec{k})]\,, \qquad (2)$$

with $iK_\mu(\vec{k})$ the Fourier transform of Δ_μ, and $K_\mu \simeq k_\mu$ at long wavelengths. The symmetric strain tensor $\underline{\underline{E}}(\vec{r})$ with $d(d+1)/2$ components describes deformations of, as well as variations between, the unit cell(s); and can be assigned to sites on the dual lattice e.g. at centroids of a square unit cell. The strain components transform as a second rank tensor: if (x, y) are coordinate variables, then clearly $E_{xx} \sim xx$, $E_{xy} \sim xy$ etc., under the unit-cell symmetry group. The physical strains are linear combinations of these.

The 1D case is of course trivial. In 2D there are $d(d+1)/2 = 3$ physical strains; compressional $e_1 = (E_{xx} + E_{yy})/\sqrt{2}$ (e.g. square to larger/smaller square); $e_2 = (E_{xx} - E_{yy})/\sqrt{2}$ (e.g. square to rectangle, along x or y directions); and shear $e_3 \equiv E_{xy} \equiv E_{yx}$ (e.g. square to equal-side parallelogram). The strains are as defined even for other transitions, and combinations of e_2, e_3 describe deformations of an equilateral to isosceles triangle [8]. In 3D (cubic lattice) there are $d(d+1)/2 = 6$ strains [9,12,14]: one compressional $e_1 = (E_{xx} + E_{yy} + E_{zz})/\sqrt{3}$; two independent deviatoric strains $e_2 = (E_{xx} - E_{yy})/\sqrt{2}$ and $e_3 = (E_{xx} + E_{yy} - 2E_{zz})/\sqrt{6}$; and three shear strains $e_4 = E_{yz}$, $e_5 = E_{xz}$, $e_6 = E_{xy}$. (Here, the numerical prefactors are conventional [17].) In the continuum limit, the discrete differences become derivatives yielding engineering strains [14], but as defined, $\underline{\underline{E}}(\vec{r})$ applies throughout Level 1. The usefulness of the unit-cell strain concept becomes clear when modeling ferroelastic structural transitions.

3. STRUCTURAL SYMMETRY AND FREE ENERGY

The network of directional bonds linking atomic bases can soften with temperature, driving structural phase transitions. In complex oxides, ferroelastic transitions can occur, with strain (Level 1) as the order parameter, and unit cells deforming in a smooth displacive manner, with the low temperature strained-cell symmetry group being a subgroup of the high temperature (zero-strain) unit-cell symmetry group [12]. The microscopic partition function will involve a trace over all the electronic and nuclear degrees of freedom (Level 3) that form the directional bonds of the atomic basis (Level 2), consistent with the strained lattice (Level 1). The resulting free energy functional F is a scalar function of the local strain tensor, with a sum over unit-cell contributions, i.e. $F = \sum_r f(\underline{\underline{E}}(\vec{r}), \vec{\Delta}\underline{\underline{E}}(\vec{r}))$. The free energy density f can be written as a series in increasing-order polynomials in the strain-tensor components, that are invariant under the *discrete* (high temperature) unit-cell symmetry group. For the square unit cell, and with $x = R\cos\theta$, $y = R\sin\theta$, examples of invariants are $e_1^2 \sim (xx + yy)^2 \sim R^2$; $e_2^2 \sim (xx - yy)^2 \sim R^2\cos^2 2\theta$; $e_3^2 \sim (xy)^2 \sim R^2\sin^2 2\theta$; and a gradient term $\vec{\Delta}e_2 \cdot \vec{\Delta}e_2 \sim R^2\cos^2 2\theta$, all unchanged under e.g. 90° rotations, $\theta \to \theta + \pi/2$. For a triangular unit cell, invariants include the cubic, $e_2^3 - 3e_2e_3^2 \sim R^3\cos 3\theta$, unchanged under 120° rotation, $\theta \to \theta + 2\pi/3$.

A first-order square to rectangle transition, with deviatoric strain order parameter $\varepsilon \equiv e_2$ positive (negative) for rectangle along the x (y) direction. The invariant polynomials up to sixth power in the order parameter can be written in scaled form [7,8] as:

$$f(e_1, \varepsilon, e_3) = \xi_o^2(\vec{\Delta}\varepsilon)^2 + f_{non}(e_1, e_2) + f_o(\varepsilon). \quad (3)$$

Here the triple-well Landau term $f_o = (\tau - 1)\varepsilon^2 + \varepsilon^2(\varepsilon^2 - 1)^2$ has minima at $\varepsilon = \pm 1$, that are degenerate with the square unit-cell $\varepsilon = 0$ minimum at scaled temperature $\tau(T) = 1$. The non-order parameter term

$$f_{non} = (1/2)A_1e_1^2 + (1/2)A_3e_3^2 \quad (4)$$

is harmonic in the compressional and shear strains. Notice that in the displacement representation, every term in Equation (3) and (4) is an anisotropic gradient of $\vec{u}$: for example, $e_3^2 \sim (\Delta_x u_y + \Delta_y u_x)^2$ is quadratic, and $\varepsilon^6 \sim (\Delta_x u_x - \Delta_y u_y)^6$ is a sixth-power, displacement gradient term. Monte Carlo simulations [16] or free energy minimizations [18], in $\vec{u}$, yield 'twin' domain walls oriented along a diagonal.

Now comes our crucial point. It is tempting to think of the strains as the physical variables in a 'strain representation' for free energy minima: then since the minima of the harmonic Equations (4) are $e_1 = e_3 = 0$, one could further minimize $f(0,\varepsilon,0)$. However, this is incorrect as strains are all components of a single, symmetric strain tensor; that moreover has too many components: $d(d+1)/2 > d$, the number of displacement degrees of freedom. There must be $N_c = d(d-1)/2$ independent constraints, to obtain the correct $d(d+1)/2 - N_c = d$ number of degrees of freedom. In fact, these required constraints for the strain representation to be consistent, do exist: they are the St. Venant compatibility conditions [13,14,15], expressing the single-valuedness of the underlying displacement field, with no defects.

4. ELASTIC COMPATIBILITY: LATTICE INTEGRITY EQUATIONS

The St. Venant compatibility equations [13,14,15] follow immediately from the strain tensor definition of Equation (2), and are

$$\vec{\Delta} \times \{\vec{\Delta} \times \underline{\underline{E}}(\vec{r})\}^T = 0 \; ; \; \vec{K} \times \underline{\underline{E}}(\vec{k}) \times \vec{K} = 0 \qquad (5)$$

where T means 'transpose'. As Baus and Lovett have noted [15], the displacement representation is similar to doing electromagnetism in terms of the vector potential $\vec{A}$, with Equation (5) then being just a vector identity analogous to $\vec{\Delta} \cdot (\vec{\Delta} \times \vec{A}) = 0$. However, once a physical field variable $\vec{B} = \vec{\Delta} \times \vec{A}$ is defined, it is illuminating to think of $\vec{\Delta} \cdot \vec{B} = 0$ as an independent field equation in a magnetic field representation. Similarly [7,8,9,11], the St. Venant constraint Equation (5) can be elevated to a field equation for the tensorial variables, in a *strain* representation.

In 2D, there are $N_c = 1$ compatibility equations [7,16]:

$$\vec{\Delta}^2 e_1 - (\Delta_x{}^2 - \Delta_y{}^2)\varepsilon - \sqrt{8}\Delta_x\Delta_y e_3 = 0\,; Q_1 e_1(\vec{k}) + Q_2\varepsilon(\vec{k}) + Q_3 e_3(\vec{k}) = 0 \qquad (6)$$

where $Q_{1,2,3}(\vec{k})$, the Fourier transforms of the difference operators, are more simply stated in their long wavelength limits, $Q_1(\vec{k}) \simeq -k^2/\sqrt{2}$; $Q_2(\vec{k}) \simeq k_x{}^2 - k_y{}^2/\sqrt{2}$; $Q_3 \simeq 2k_x k_y$.

If we substitute $e_1(\vec{k}) = -[Q_2\varepsilon(\vec{k}) + Q_3 e_3(\vec{k})]/Q_1$ into $f_{non}(e_1, e_3)$ of Equations (3), (4), then compatibility is satisfied for *any* $\varepsilon(\vec{k})$, $e_3(\vec{k})$. Minimizing with respect to $e_3(\vec{k})$ [19] yields non-OP strains in terms of the OP strain $e_{1,3}(\vec{k}) = B_{1,3}(\vec{k})\varepsilon(\vec{k})$, and so the free energy density of Equation (3) is entirely in terms of the OP strain. The harmonic non-OP cost becomes a *nonlocal* PLA compatibility potential term, $f_{non}(e_1, e_3) \equiv f_{compat}(\varepsilon)$ so Equation (3) becomes

$$f(\varepsilon) = \xi_o{}^2(\vec{\Delta}\varepsilon)^2 + f_{compat}(\varepsilon) + f_o(\varepsilon)\,, \qquad (7a)$$

where in Fourier space

$$f_{compat} = (1/2)[A_1 |B_1(\vec{k})|^2 + A_3 |B_3(\vec{k})|^2]\,|\varepsilon(\vec{k})|^2 \equiv (1/2)A_1 U(\vec{k})\,|\varepsilon(\vec{k})|^2 \qquad (7b)$$

and in coordinate space $f_{compat} = (1/2)A_1 U(\vec{r} - \vec{r}')\varepsilon(r)\varepsilon(r')$. The compatibility kernel for the 2D square-rectangle transition is (with $D(\vec{k}) \equiv Q_3{}^2 + (A_3/A_1)Q_1{}^2$):

$$U(\vec{k}) = \frac{(A_3/A_1)Q_2{}^2}{D}; e_1(\vec{k}) = -\frac{(A_3/A_1)Q_2 Q_1\varepsilon(\vec{k})}{D}; e_3(\vec{k}) = -\frac{Q_2 Q_3\varepsilon(\vec{k})}{D}\,. \qquad (8)$$

The free energy minima can be found by a relaxational OP dynamics [8] $\partial\varepsilon/\partial t = -\partial F/\partial\varepsilon$ with initial conditions $\varepsilon(\vec{r}, t=0)$ random, with zero mean. In this (OP) strain representation, the $\varepsilon(\vec{r})$ variables are 'effective scalars' at each site, with anisotropy of the fourfold unit-cell symmetry

carried entirely by the compatibility potential $U(\vec{r}-\vec{r}') \sim \cos 4(\theta-\theta')/|\vec{r}-\vec{r}'|^2$ where $\hat{r}\cdot\hat{r}' = \cos(\theta-\theta')$. The power law decay $\sim 1/R^d$, is faster than Coulombic (or critical correlation-like) fall-off $\sim 1/R^{d-2}$, and arises generically from the Fourier transform of kernels as in Equation (8) that for long wavelengths are independent of $|\vec{k}|$ since they depend only on *ratios* $Q_{2,3}/Q_1$: as $U(\vec{k}) \simeq U(\hat{k})$, one has $\int d^d k e^{i\vec{k}\cdot\vec{R}} U(\vec{k}) \sim 1/R^d$. Since the angular average of $U(\vec{R})$ is zero, the influence of arbitrary strain variations could fall off even faster.

Each ferroelastic transition has its own characteristic compatibility kernel, that can be evaluated in 2D [7,8,12,16] and 3D [9]. The sign variation with direction of $U(\vec{r}-\vec{r}')$ implies local strain has 'ferro/antiferro' (elastic) frustration, that tends to favour spatial strain texturing, or patterns of domain walls. Since $\sum_r f_{compat} > 0$ from its origin in Equation (4), for $A_1 \gg 1$ the St. Venant forces exert a strong orientational effect on domain walls, to reduce the local non-OP strains as much as possible. From Equation (8), $U(k) \sim (k_x^2 - k_y^2)^2$ so $\hat{k}_x \pm \hat{k}_y$ or $\pm\pi/4$ orientation domain walls are favoured for the square-rectangle transition with consequent expulsion of non-OP strains as $e_{1,3}(\vec{k}) \sim k_x^2 - k_y^2 \sim 0$ in an 'elastic Meissner effect' [7]. (For the triangle-rectangle transitions, the kernel favours three $2\pi/3$ orientation domain walls meeting at a point, around which the non-OP compressional strain is concentrated [8], as required for lattice integrity.) kernels in 3D induce complex helical texturing [9].

Domain walls N_{dom} of thickness ξ_o, across system size L_o, will reduce the bulk energy $-D_o L_o^2$ (where D_o is an elastic energy density) in a strip $\xi_o L_o$ and have a 'gradient squared' energy cost, so the textured-state energy is $-D_o[L_o^2 - N_{dom}\xi_o L_o] + D_o N_{dom}\xi_o^2(1/\xi_o^2)\xi_o L_o$. This is a fractional energy difference of only $\delta \equiv 2N_{dom}(\xi_o/L_o)$ above the uniform $N_{dom} = 0$ state [20]. (For equal-width twins of separation $W \sim L_o^{1/2}$ [7], and $N_{dom} = L_o/W$ textured state, the difference $\delta \sim 1/L_o^{1/2}$.) In general, the uniform 'true' ground state is only one out of many asymptotically degenerate competing textured states, and the latter will be favoured, on quenching from an arbitrary initial state, especially as ferroelastic dynamics

favours an early lock-in of large wave-vector textures [8]. For doped ferroelastics, charges and spins acting as local internal stresses and temperatures can make structural heterogeneity the preferred state.

5. COUPLING TO CHARGES AND SPINS

External stress, locally applied, can have *nonlocal* static effects in ferroelastics (see Fig. 4 of Ref. [7]). Dynamical evolution of strains under local external stress can show striking time-dependent patterns such as 'elastic photocopying' of the applied deformations, in an expanding texture (see Fig.5 of Ref. [8]). Since charges and spins can couple linearly to strain, they are like *internal* (unit-cell) local stresses, and one might expect extended strain response in *all* (compatibility-linked) strain-tensor components. Quadratic coupling is like a local transition temperature. The model we consider is a (scalar) free energy density term

$$f_{coupling} = A_{n1} n e_1 + A_{m1} m^2 e_1 + A_{n\varepsilon} n \varepsilon^2 + A_{nm} n m^2 , \tag{9}$$

where $n(\vec{r})$ is a sum of doped-charge number densities with an exponential profile $\exp(-|\vec{r}-\vec{r}_i|)$, with unit-cell extent around site $\vec{r}_i$. The magnetization variable $m(\vec{r})$ is the staggered magnetization for cuprates, and the (core-level) ferromagnetic moment for manganites, with

$$f_{mag} = d_o[\xi_m (\vec{\Delta} m)^2 + (T - T_{cm}) m^2 + (1/2) m^2] , \tag{10}$$

where d_o is a magnetic/elastic energy ratio; T_{cm} is a nonzero scaled Ne'el temperature for 'cuprates'; and $T_{cm} = 0$ for 'manganites' (purely paramagnetic parent compound). The constants $A_{n1}, A_{m1}, A_{n\varepsilon}, A_{nm}$ are chosen to mimic cuprates (manganites), e.g. $A_{nm} > 0$, ($A_{nm} < 0$), representing a suppressing (inducing) of magnetization by the hole-doped mobile charges. In a relaxational dynamics ($\partial \varepsilon / \partial t = -\partial F / \partial \varepsilon$, $\partial m / \partial t = -\partial F / \partial m$) and $f = f_{grad} + f_o + f_{compat} + f_{coupling} + f_{mag}$, with fixed charges randomly placed, we obtain $\varepsilon(\vec{r}), e_1(\vec{r}), m(\vec{r})$ textures [10,11].

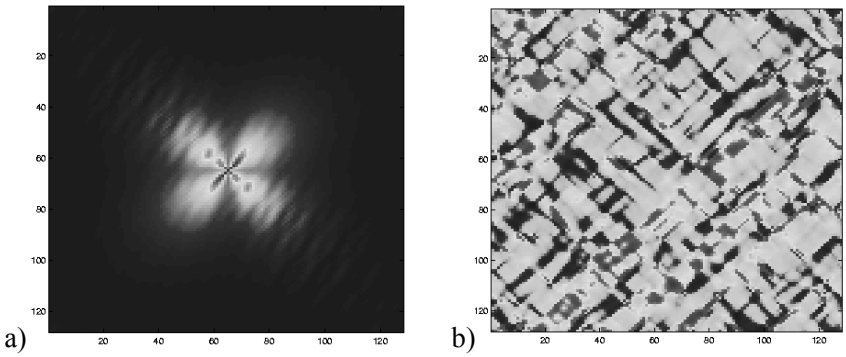

Figure III:3:1. a) Single 'cuprate' pemton greyscale plot of deviatoric strain $|\varepsilon(\vec{k})|^2$ in Fourier space. b) Multipemton greyscale deviatoric strain $\varepsilon(\vec{r})$ plot in coordinate space for hole-doped 'mobile' charges fraction x = 0.1.

The textured polaron in $\varepsilon(\vec{r})$ that results, extends over tens of lattice spacings, with a fourfold symmetry from the PLA compatibility potential also reflected in Fourier space, Fig. 1a), cuprate case. Similar quadrupolar patterns occur in other coupled variables, and we term the excitation as a '*p*olaronic *e*lasto-*m*agnetic *t*exture' or '*pemt*on'. Fig 1b) shows diagonal stripe-like [3] textures for random doping fraction $x = 0.1$: the multipemtons are not rigid, but mutually deform each other. To get a complete picture both coordinate and Fourier space plots are necessary, and the logscale Fourier plots ($|\varepsilon(\vec{k})|^2, |m(\vec{k})|^2$) in Ref [11] reveal $\vec{k} \to -\vec{k}$ inversion symmetry even in fine details. The fourfold butterfly-like plots in experimental diffuse X-ray scattering in manganits and cuprates [21] (and their cross-response to a magnetic field) could possibly reflect such pemton signatures. Our model's multipemton textures show both direct and cross-responses, and at multiple scales: a long wavelength external magnetic field (stress) produces short-wavelength 'cloud-like' [5] gradations in strain (magnetization) [22]. This is similar to experiment [4,5,6] and occurs because of nonlinearity, with $\varepsilon^6(r) \to \prod_{s=1}^{6} \varepsilon_{qs}$, $m^4(r) \to \prod_{s=1}^{4} m_{qs}$ in Fourier space coupling wavevectors for different scales.

Charge and strain couple to magnetization quadratically ($\sim m^2$) and act as local variations of the transition temperature: from Equation (9) and (10), $T_{cm}'(r) = T_{cm} - (A_{m1}e_1 + A_{nm}m)/d_o$. Thus at a given T, some regions will be

below, $T - T_{cm}'(r) < 0$ (above, $T - T_{cm}'(r) > 0$) transition, with $m^2(\vec{r}) \neq 0$ ($m^2(\vec{r}) = 0$), as seen in the large-fluctuation $m(\vec{r})$ (flat $m(\vec{r}) = 0$) regions in Fig. 2 of Ref. [10]. For manganites ($T_{cm} = 0$, paramagnetic parent) at low doping the spatial average $< m >= 0$ until a threshold doping x_c is reached when symmetry-breaking $< m > \neq 0$ occurs in these nonzero $m^2(\vec{r})$ regions. For warming at fixed $x \equiv < n >$, the flat $m(\vec{r}) = 0$ regions expand and $< m >$ decreases. Thus there is doping and temperature-dependent *annealed and correlated percolation*: this differs from quenched-disorder scenarios [1]. For cuprates ($T_{cm} \neq 0$), the model suggests the Ne'el temperature transition could have a percolative character.

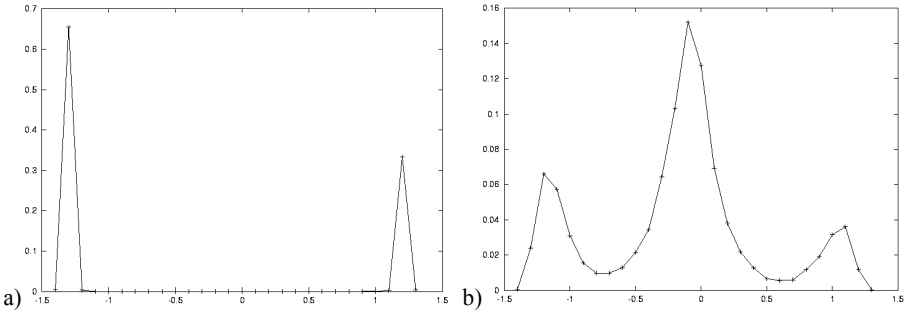

Figure III:3:2. a) For the 'twinned' parent compound, x=0, probability of finding a deviatoric strain $\varepsilon(\vec{r})$ versus the strain. b) Similar plot for x=0.1 multipemton strain

Fig. 2(a) and 2(b) show further results not presented in Ref. [10]: the probabilities of finding (positive/negative) strains of a given value show a double-hump behaviour. From the charge-strain couplings one might expect single-sign strains. However, *both* signs of deviatoric strain (and *both* compression and dilatation) occur, in energy-lowering 'adaptive elastic screening' [11]. For cuprates and manganites, bimodal distributions of interatomic distances are experimentally seen [3,23]. Although our model here [10] has fixed charges, an extension to allow hopping would result in charge ordering through $U(\vec{R})$ mediated charge-charge PLA forces.

Finally we comment that adding isotropic Coulomb forces should not destroy the essential features of the anisotropic intrinsic heterogeneity here

induced by St. Venant forces alone. Conversely, any consistent calculation of dissipative response (e.g. resistivity) from Coulombic plus phononic scattering in the displacement representation will be unchanged by working in the strain representation, as the PLA elastic forces are already implicit in the generic assumption of lattice integrity, for both representations. Such compatibility contributions can be large for materials with widely differing strain-component energy scales, e.g. with dimensionless elastic constant $A_1 \gg 1$[8]. This anisotropic (Level 1) parameter regime could be accessible in complex compounds with anisotropic (Level 2) atomic bases, e.g. in transition-metal oxides with perovskite octahedra' comprised of directionally bonded ions and deformable/polarizable oxygens. It is the interplay between strain nonlinearity, elastic compatibility, and multivariable couplings that drives the multiscale intrinsic heterogeneity of cuprates, manganites, and other complex adaptive materials.

REFERENCES

1. E. Dagotto, (Ed.) Nanoscale Phase Separation and Colossal Magnetoresistance, Springer (2003).
2. A.R. Bishop, S.R. Shenoy and S. Sridhar (Eds.) Intrinsic Multiscale Structure and Dynamics in Complex Electronic Oxides, World Scientific (2003).
3. A. Bianconi, N.L. Saini, A. Lanzara, M. Missori, T. Rosetti, H. Oyanagi, H. Yamguchi, K. Oka and T. Ito, Phys. Rev. Lett. 76, 3412 (1996); E.S. Bozin, G.H. Kwei, H. Takagi and S.J.L. Billinge, Phys. Rev. Lett. 84, 5856 (2000); K.M. Lang, V. Madhavan, J.E. Hoffman, E.W. Hudson, H. Eisaki, S. Uchida and J.C. Davis, Nature 415, 412 (2002).
4. Y. Huang, I.M. Palstra, S.W. Cheong and B. Batlogg, Phys. Rev. B 52, 15046 (1995)
5. M. Faeth, S. Friesen, A.A. Menovsky, Y. Tomloka, J. Aarts and J.A. Mydosh, Science 285, 1540 (1999).
6. Y. Ando in Ref. [2].
7. S.R. Shenoy, T. Lookman, A. Saxena and A. R. Bishop, Phys. Rev. B 60, R12537 (1999).
8. T. Lookman, S. R. Shenoy, K.O. Rasmussen , A. Saxena and A.R. Bishop, Phys. Rev. B, 67, 024114 (2003); T. Lookman, S. R. Shenoy, K.O. Rasmussen, A. Saxena and A.R. Bishop, J. de Physique IV, ICOMAT-02 Proc. (2003).
9. K.O. Rasmussen, T. Lookman, A. Saxena, A.R. Bishop, R. C. Albers and S.R. Shenoy, Phys. Rev. Lett. 87, 055704 (2001).
10. A.R. Bishop, T. Lookman, A. Saxena and S.R. Shenoy, Europhysics Lett. 63, 289 (2003).

11. S.R. Shenoy, T. Lookman, A. Saxena and A.R. Bishop, in Ref. [2].
12. A. Saxena, T. Lookman, A.R. Bishop and S.R. Shenoy, in Ref. [2]; D.M. Hatch, T. Lookman, A. Saxena and S.R. Shenoy, Phys. Rev. B 68, 104105 (2003).
13. A.J.C. Barre de Saint-Venant in C.L.M.H. Navier, Resume' des Lecons sur l'Application de la Mechanique (Dunod, Paris, 1864).
14. S.F. Borg, Fundamentals of Engineering Elasticity, Second edn. 1990, World Scientific.
15. M. Baus and R. Lovett, Phys. Rev. Lett. 65, 1781 (1990); 67, 406 (1991); Phys. Rev. A 44, 1211 (1991).
16. S. Kartha,, J.A. Krumhansl, J.P. Sethna and L.K. Wickham, Phys. Rev. B 52, 803 (1995).
17. The 'normalization' factors are chosen so that for e_1, e_2 in 2D $(E_{xx}^2 + E_{yy}^2)/2 = 1$; or for e_3 in 3D, $(4E_{xx}^2 + E_{yy}^2 + E_{zz}^2)/6 = 1$, at $|E_{xx}| + |E_{yy}| + |E_{zz}| = 1$.
18. A.E. Jacobs, Phys. Rev. B 52, 6327, (1995).
19. This direct method yields the same results as the Lagrange multiplier method for finding the kernel introduced in Ref. [16] for the square-rectangle case, and used for kernels in 2D and 3D in Refs. [7-12].
20. In Fig. 8 of Ref. [8], different nearly-degenerate textured states evolved under relaxational dynamics are shown. In scores of such relaxations, we have found a uniform state only once, for a particular initial-state random seed.
21. L. Vasiliu-Doloc, S. Rosenkranz, R. Osborn, S.K. Sinha, J.W. Lynn, J. Mesot, O.H. Seeck, G. Preost, A.J. Fedro and J.F. Mitchell, Phys. Rev. Lett. 83, 4393 (1999); S. Shimomura, N. Wakabayashi, H. Kuwahara and Y. Tokura, Phys. Rev. Lett. 83, 4389 (1999); Z. Islam, X. Liu, S.K. Sinha, J.C. Lang, S.C. Moss, D. Haskel, G. Srajer, P. Wochner,D.R. Lee, D.R. Haeffner and U. Welp, Phys. Lett. 93, 157008 (2004).
22. A.R. Bishop, T. Lookman, A. Saxena and S.R. Shenoy, cond-mat/0304198.
23. Ch. Renner, G. Aeppli, B-G. Kim, Y-A. Soh, and S.W.Cheong, Nature 416, 518 (2002); S.J.L. Billinge in Ref [2].